Research in Veterinary Science 191 (2025) 105690

Contents lists available at ScienceDirect

Research in Veterinary Science

journal homepage: www.elsevier.com/locate/rvsc

Stereological and morphometric insights into epididymal development in domestic cats (*Felis silvestris catus*) from 6 to 48 months

P. Salinas *, D. Escobar

Laboratory of Animal & Experimental Morphology, Institute of Biology, Faculty of Sciences, Pontificia Universidad Católica de Valparaíso, Valparaíso, Chile

ARTICLE INFO

Keywords:
Epididymis
Epididymal duct
Age
Histology
Stereology
Morphometry

ABSTRACT

This study characterizes age-related morphometric and morphological changes in the epididymis of domestic cats (*Felis silvestris catus*) from puberty to adulthood (6 to 48 months), emphasizing its essential role in sperm maturation and storage—key processes for male fertility. A total of 42 epididymides were analyzed using histological staining (hematoxylin-eosin) and stereological quantification through the STEPanizer software. Morphometric analyses revealed an age-dependent increase in the diameter of the epididymal duct and epithelial height in the *caput*, whereas the *cauda* exhibited a progressive reduction in epithelial height, possibly reflecting adaptations in sperm storage capacity during sexual maturation. Morphological observations showed the presence of intraepithelial cysts in cats aged 24 to 48 months, along with the consistent detection of spermatozoa in all regions and age groups. Stereological findings indicated an increased volumetric density (%VV) of the ductal epithelium, particularly in the *caput* between 6 and 12 months of age, supporting the influence of androgenic activity on regional epididymal maturation. These changes suggest dynamic, age-related structural remodeling of the epididymal parenchyma, especially in epithelial and luminal components. While this cross-sectional study—conducted during the southern hemisphere spring—provides valuable insights into epididymal development, its design limits the establishment of causal relationships between age and histological changes. Future longitudinal studies examining hormonal modulation of epididymal maturation in domestic cats are encouraged. Overall, these findings contribute foundational knowledge of feline reproductive anatomy and underscore the importance of the epididymis as a hormonally responsive organ central to male fertility.

1. Introduction

The study of reproductive function in domestic cats (*Felis silvestris* catus) is pivotal due to their unique role as models bridging domestic and wild felids, offering insights into reproductive biology with implications for conservation and reproductive biotechnology (Sowińska, 2021). Their phylogenetic proximity to endangered wild felids underscores their value in understanding morphological and functional changes in the epididymis during early life stages, which are critical for fertility and species preservation (Pintus et al., 2021). While histological characteristics of the cat epididymis are documented, decaudaed morpho-quantitative analyses of postnatal development remain scarce. Previous studies have reported age-related histological changes in veterinary medicine, such as lipofuscin deposition in ductuli efferentes cells, interstitial fibrosis, tubule dilatation with epithelial flattening and loss of stereocilia, epithelial hyperplasia, spermatic granulomas, and regenerative responses like intraepithelial cyst formation (Johnson and Neaves, 1981). A study of 42 pairs of testes and epididymides from cats of varying ages identified significant changes, including tunica adventitia thickening and epithelial hyperplasia, with younger cats showing a higher incidence of intraepithelial cysts and hyperplasia, highlighting the importance of early developmental stages. However, existing research, including structural, histological, and immunohistochemical studies (Malmqvist, 1978; Axnér et al., 1999; Axnér, 2006; Sánchez et al., 1998), has largely provided qualitative descriptions focused on adult or postpubertal stages, leaving a critical gap in quantitative data on early epididymal development (Pintus et al., 2021). The epididymis, a crucial tubular organ, facilitates spermatozoa storage, maturation, and transport from the testis to the ductus deferens. Its three anatomical regions—*caput, corpus*, and *cauda*—exhibit distinct histological features tied to their functions. The caput, with its pseudostratified epithelium and stereociliated principal cells, drives sperm maturation and fluid modification, concentrating the high-volume fluid from the rete testis, while the *corpus* continues this process, and the cauda, with a lower

* Corresponding author at: Av. Universidad #330 Curauma, Valparaíso, Chile.
E-mail address: paulo.salinas@pucv.cl (P. Salinas).

https://doi.org/10.1016/j.rvsc.2025.105690
Received 5 January 2025; Received in revised form 13 April 2025; Accepted 4 May 2025
Available online 5 May 2025

epithelium, stores mature spermatozoa until ejaculation (James et al., 2020a, b). These functions are tightly regulated by hormones. Testosterone, produced by testicular interstitial endocrine cells, sustains epithelial integrity and modulates luminal fluid composition, directly influencing morphometric traits like ductal epithelium volume. Estrogens support fluid reabsorption, refining sperm maturation, while peptide hormones such as relaxin and insulin regulate sperm transport, potentially affecting regional structural differences (Smith and Walker, 2014). This hormonal interplay suggests a dynamic relationship between endocrine regulation and the morphometric and functional changes during epididymal development, yet its specific impact in domestic cats remains underexplored. To address these gaps, this study provides a novel quantitative analysis of epididymal development in domestic cats during their first 48 months of life, a period marked by significant morphological transitions. Although age-related histological changes have been documented, the lack of decaudaed morphometric data limits our understanding of how these changes correlate with sexual maturation across the *caput, corpus*, and *cauda*. The hormonal regulation by testosterone, estrogens, relaxin, and insulin further complicates this developmental process, warranting a focused investigation. Thus, we hypothesize that age significantly influences epididymal structure, with distinct regional variations in the *caput*, *corpus*, and *cauda* during the first 48 months. Our objective is to characterize these age-related morphometric changes in domestic cats between 6 and 48 months, emphasizing volumetric density of the ductal epithelium and its link to sexual maturation. Transitional insights from general epididymal function to this specific feline focus reveal a need for such data to advance reproductive biology and feline health. However, the cross-sectional design of this study limits causal inferences between age and morphological changes, a constraint we acknowledge. By quantifying these developmental patterns, our findings aim to enhance knowledge of epididymal anatomy, laying a foundation for future research in feline reproductive health and biotechnology applications.

2. Materials and methods

2.1. Ethics statement

All animal handling was in strict accordance with the NIH Guidelines for the Care and Use of Laboratory Animals (National Research Council (US) Committee, 2011) and Chilean Law 20.380.

2.2. Animals and samples

A total of 42 testes and epididymides from 42 healthy, hormone therapy-naive domestic cats of non-specific breed (*Felis silvestris catus*) were collected from the scrotal cavity during surgical castration procedures at a local Animal Hospital. The health status of each cat was confirmed through pre-surgical clinical evaluations conducted by licensed veterinarians, which included physical examinations to assess general condition, body temperature, heart and respiratory rates, and the absence of clinical signs of systemic or reproductive disease. Additionally, owners provided medical histories, and veterinary records were reviewed to ensure no prior diagnoses of chronic illnesses, infections, or reproductive abnormalities. Exclusion criteria included cats with evidence of testicular or epididymal abnormalities (e.g., cryptorchidism, masses, or inflammation), recent illness, or a history of hormonal treatments. The body weights of cats were recorded prior to surgery to further monitor overall health. To control for seasonal variations, all samples were collected during the southern hemisphere spring (October, Region of Valparaíso, Chile, 32°02′ S - 33°57′ S latitude, and 70° - 72° W longitude). Epididymides were categorized by age into groups: 6, 7, 8, 9, 12, 24, and 48 months (six epididymides per age group). The determination of age in domestic cats was carried out using criteria aimed at maximizing accuracy. Birth dates reported by owners were corroborated with veterinary hospital records, including clinical histories and vaccination schedules, which are widely accepted as reliable indicators of chronological age. However, we recognize the limitations discussed in the literature concerning the precise aging of cats beyond 8 months of age (Fleming et al., 2021). To strengthen reliability, dental wear patterns were used as a secondary reference when available. Nonetheless, we acknowledge that age classification may involve a degree of uncertainty, particularly when distinguishing individuals within close age intervals (Bellows et al., 2016). This potential limitation has been considered in the interpretation of our results. Each sample included one testis and one epididymis, with no visible abnormalities detected during macroscopic examination post-collection. Prior to fixation, the volumes of the testis and epididymis were measured. Additionally, to mitigate the effect of tissue shrinkage on the epididymal ducts, luminal diameters were determined in fresh epididymides using confocal microscopy, which allowed for high-precision imaging without fixation-related artifacts. Subsequently, to ensure adequate histological processing of cat epididymides, the tissue was collected and processed within a maximum of 30 min. The epididymides were fixed immediately after surgical removal in 10 % formalin (4 % formaldehyde) for 24 h at room temperature (22 °C).

2.3. Tissue preparation

To adjust the methodology and account for variations in the shrinkage artifact of epididymal tissue, we calibrated the microtome block advance by measuring the change in block height divided by the number of sections cut, ensuring an accurate estimate of the average section thickness (Gundersen et al., 1988; Dorph-Petersen et al., 2001; Tschanz et al., 2011). To ensure reproducibility in tissue processing, fixation was standardized by immersing all epididymal samples in 10 % formalin (4 % formaldehyde) immediately after surgical collection, maintaining a consistent fixation time of 24 h at a controlled room temperature of 22 °C. To minimize potential variations, samples were processed in small batches (no more than five at a time), and fresh formalin was used for each batch to prevent degradation of fixation quality. Temperature fluctuations were avoided by storing samples in a temperature-regulated laboratory environment, with regular monitoring to ensure consistency. Additionally, we used a systematic uniform random sampling (SURS) method to measure section thickness at different positions, employing a micrometer to record the vertical movements of the microscope stage. The SURS method was implemented by selecting random starting points within each histological section and systematically sampling at evenly spaced intervals (every 20 μm) across the tissue, ensuring unbiased representation of the entire epididymal sample. This methodology allowed us to adjust volumetric density calculations and other morphometric measurements to correct for any bias introduced by differential section shrinkage. To derive correction coefficients for tissue shrinkage, we compared measurements of luminal diameters taken immediately after dissection (using a confocal microscope for precise three-dimensional imaging of fresh, unfixed ducts) with those obtained after fixation and histological processing. The correction coefficient was calculated as the ratio of post-fixation to pre-fixation measurements, averaged across multiple samples, and validated against established shrinkage data from prior studies (Dorph-Petersen et al., 2001). This coefficient was applied to adjust stereological estimates, ensuring accuracy. Finally, we employed oil immersion objectives to minimize optical biases and ensure accurate distance measurements along the z-axis. These methodological adjustments ensured that stereological estimates were unbiased, even in the presence of tissue shrinkage. Additionally, different fixation techniques were compared to assess their impact on the preservation of duct morphology. We estimated volume deformation by comparing the sum of block volumes before and after embedding and calculated area deformation by comparing the section areas before and after sectioning. Additionally, local section thickness measurements were taken for each counting frame, allowing us to weight the calculations appropriately.

These steps ensured that our stereological estimates remained unbiased, even with differential shrinkage among specimens. Based on the regional epididymal classification proposed by Axnér et al. (1999), specific sections were extracted from the *caput* (head; regions 1 and 2), *corpus* (body; region 5), and *cauda* (tail; region 6; Fig. 1A).

2.4. Histological processing and correction of shrinkage artifacts

Once fixed, the epididymides were dehydrated through a graded ethanol series, cleared with xylene, and embedded in Paraplast (embedding medium: Paraplast Plus; melting point: 54 °C; Sigma-Aldrich Chemical Co., St. Louis, MO, USA). Tissue sections of 5 μm thickness were obtained using a motorized rotary microtome (Leica RM2255, Leica Microsystems, Switzerland). The sections were then rehydrated, treated with xylene for 10 min, and gradually hydrated through decreasing ethanol concentrations (100 %, 96 %, 80 %, and 70 %, each for 15 s), followed by distilled water. Histological cross-sections of the epididymis were routinely stained with hematoxylin and eosin and scanned using a Motic Easy Scan Pro® digital slide scanner (Motic Instrument Inc., Canada) to generate full panoramic views. As this study is both descriptive and quantitative, only hematoxylin-eosin staining was used, as it facilitates digital image analysis and numerical data extraction. To refine the methodology and account for tissue shrinkage artifacts in the epididymis, microtome block advance was calibrated by measuring the change in block height divided by the number of sections cut, ensuring accurate estimation of the average section thickness (Gundersen et al., 1988; Dorph-Petersen et al., 2001; Tschanz et al., 2011). A systematic uniform random sampling method was also used to measure section thickness at various positions, with a micrometer used to record vertical stage displacements on the microscope. Oil immersion objectives were employed to minimize optical distortion and ensure accurate z-axis distance measurements. This methodology allowed us to correct potential biases caused by tissue shrinkage, ensuring both precision and unbiased stereological estimations (Dorph-Petersen et al., 2001). To further mitigate the effects of shrinkage on epididymal ducts, luminal diameters were remeasured after fixation and histological processing and compared to values obtained from fresh tissue. A correction factor, derived from previous studies on tissue contraction, was then applied to adjust final measurements. In addition, different fixation techniques were evaluated to assess their influence on the preservation of ductal morphology. Volumetric deformation was estimated by comparing the total volume of tissue blocks before and after embedding, while area deformation was calculated by comparing section areas before and after sectioning. Local section thickness was also measured in each counting frame, allowing for weighted and accurate stereological calculations. These procedures ensured that the stereological estimates remained unbiased, even in the presence of differential tissue shrinkage among specimens.

2.5. Morphological and stereological analysis

Histological sections from all 42 epididymides (six per age group: 6,

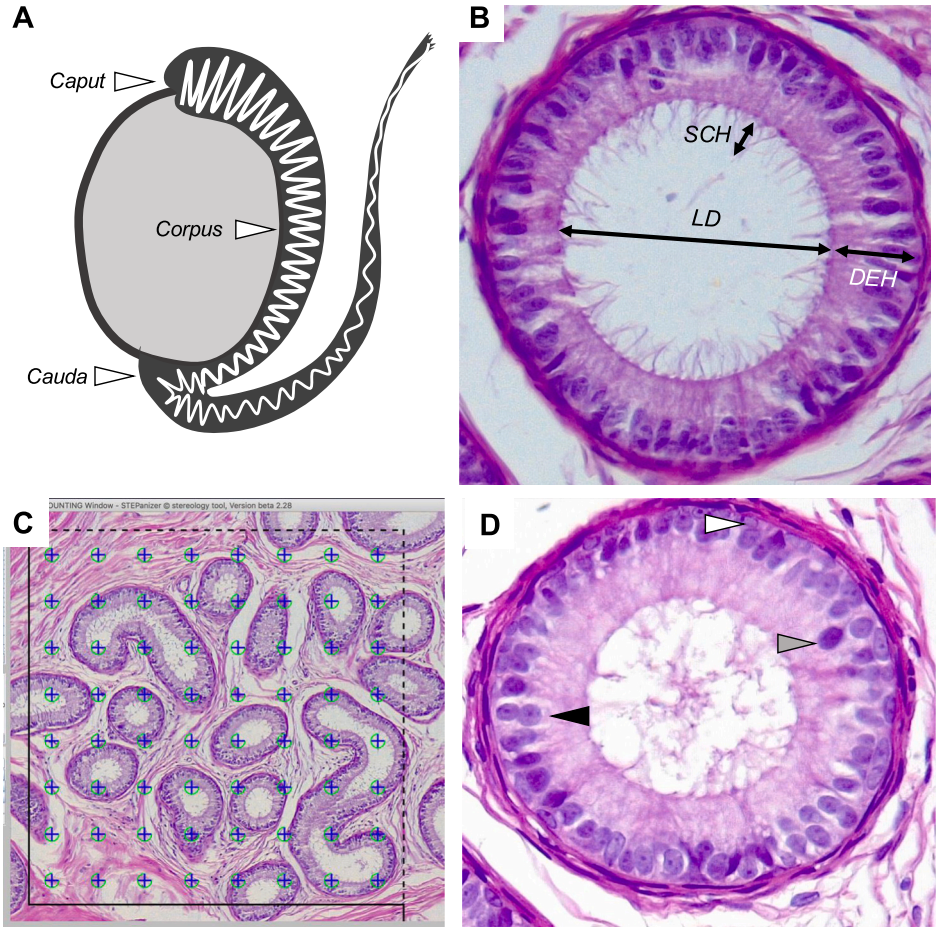

Fig. 1. A, Diagram of testis and epididymis in domestic cats (*Felis silvestris catus*), shows the site for obtaining histological sections. B, Linear morphometric variables were measured in epididymal duct (*Ductus epididymidis*): lumen diameter (LD), ductal epithelium height (DEH), stereocilia height (SCH). C, M_{64} STEPanizer Test System interface used to quantify volume density (V_V estimated by point counting; %) of ductal area, smooth muscle, connective tissue, ductal epithelium and blood vessels. All the stereological parameters were estimated by light microscopy at 20×. D, Type of epithelial cell in epididymal duct photomicrograph, basal (*white arrow*), principal (*black arrow*) and apical (*gray arrow*) cells (Hematoxylin-Eosine, 40×).

7, 8, 9, 12, 24, and 48 months) were analyzed. The linear morphometric variables evaluated in the *caput*, *corpus*, and *cauda* of the *ductus epididymidis* included luminal diameter (LD; defined as a transverse line connecting two opposing points at the apical margin of the ductal epithelium, measured exclusively in ducts exhibiting a circular profile), ductal epithelial height (DEH; measured as a perpendicular line from the base to the apical membrane of the epithelium), and stereocilia height (SCH; measured from the apical plasma membrane to the distal end of the stereocilia; see Fig. 1B). The morphometric description was carried out by simple observation, analyzing four quadrants per field. All measurements were performed at 40× magnification. For the stereological analysis**,** unbiased sampling and acquisition of estimators were conducted as described by Geuna and Herrera-Rincon (2015). Five microscopic fields were examined per epididymal region (*caput*, *corpus*, and *cauda*), totaling 15 fields per epididymis. Panoramic digital images of the entire tissue section were obtained using a digital slide scanner, and additional high-magnification (40×) images were acquired as needed for detailed quantification. All samples within each age group underwent identical morphometric and stereological assessments to ensure consistency. Measurements in the *caput*, *corpus*, and *cauda* were performed independently of a predefined order, and the sequence of regional analysis was randomized to prevent systematic bias. This approach eliminated order-related confounding in the data collection process. Histological sections (5 μm thick, with 20 μm intervals) were prepared and analyzed per region. Stereological estimations were performed in five microscopic fields per sample (Gundersen et al., 1988). Volume densities (%VV) for the ductal lumen (DLA), smooth muscle (SM), connective tissue (CT), ductal epithelium (DE), and blood vessels (BV) were quantified under 10× magnification using the M64 test system of the STEPanizer Stereological Tool, which included 64 test points, a test line of 18d, and a test area of $36.36d^2$ (Tschanz et al., 2011; see Fig. 1C). Images from all age groups were systematically reviewed, and stereological assessments incorporated corrections for tissue deformation (Dorph-Petersen et al., 2001). All measurements were carried out independently by two trained observers using the same microscopy system, and the observers were blinded to the experimental groups. Epithelial cell types were identified by visual inspection (Fig. 1D), analyzing five ducts per region and quantifying 100 nuclei per duct to determine the proportions of principal, apical, and basal cells, following standardized criteria (Gundersen et al., 1988; Tschanz et al., 2011; Dorph-Petersen et al., 2001). A preliminary training phase was conducted prior to data collection to standardize classification criteria. Manual point counting and cell recording were performed using printed acetate grids at 10× and 40× magnification. Computational corrections were not applied to linear measurements such as tubular diameter, luminal diameter, or epithelial height. Prior to stereological analysis, a verification step was implemented to validate the accuracy and reliability of the quantitative data (Dorph-Petersen et al., 2001). A constant fraction of the section thickness was sampled to mitigate potential bias due to tissue shrinkage. Section thickness was measured at multiple sites to ensure that the coefficient of error (CE) remained below 5 %, consistent with methodological guidelines. All anatomical and histological terms employed in this study adhered to the *Nomina Histologica Veterinaria* (International Committee on Veterinary Gross Anatomical Nomenclature (ICVGAN), 2017) and *Nomina Anatomica Veterinaria* (International Committee on Veterinary Histological Nomenclature (ICVHN), 2017), thereby ensuring terminological accuracy and consistency throughout the manuscript.

2.6. Statistical analyses

Epididymis data was recorded on Microsoft Excel for Mac OS X (Microsoft Corporation) and exported to GraphPad Prism 8.0 software for Mac OS X (GraphPad Software, San Diego, CA) to generate descriptive statistics. Multiple measurements from the same individual were averaged before performing statistical analyses to ensure that each individual contributed a single representative value per variable. All data were ordered according to age and expressed as mean ± standard deviation (SD). The D'Agostino-Pearson test was used to evaluate data normality. To address potential outliers, we inspected data distributions using boxplots and applied the ROUT method (Q = 1 %) in GraphPad Prism to identify and evaluate outliers, retaining them unless they were attributable to clear experimental errors (e.g., measurement or recording issues), which occurred in fewer than 2 % of cases. No data transformations were applied, as the D'Agostino-Pearson test confirmed normality for most variables, and non-normal datasets were analyzed using robust statistical methods where appropriate. To observe the effect of age on linear morphological variables of the epididymal duct, a one-way ANOVA followed by Tukey's post-test for multiple comparisons was used. To test whether slopes and intercepts (corpus weight, epididymis, and testis volume) were significantly different, a simple linear regression was performed with 95 % confidence intervals. Additionally, an r-Pearson correlation test was conducted between stereological variables; these calculations were performed after computing the mean of side-by-side replicates and analyzing those means. Statistical significance for all hypothesis tests was set at $p < 0.05$.

3. Results

3.1. Morphological changes in the epididymis

All domestic cats appeared healthy during sampling for this study. According to the owners, the cats were not exposed to endocrine disruptors. The epididymis of cats across all assessed age groups was surrounded by a thin layer of loose connective tissue containing collagen fibers, fibroblasts, and blood vessels, providing structural support without forming a distinct capsule (Fig. 2). Histological analysis revealed spermatozoa populations in all three epididymal regions by six months of age, with the cauda showing the highest concentration of spermatozoa in the ductal lumen. By eight months, increased spermatozoa presence was observed across all segments, with notable agglutination of spermatozoa in the *caput, corpus,* and *cauda* by twelve months, as observed in hematoxylin-eosin-stained sections. This development in the domestic cat's epididymis during the first year shows a direct correlation with the presence and concentration of spermatozoa. Both pseudostratified and simple cuboidal epithelia were noted in the caput at all ages, except in 24-month-old cats, which exclusively showed pseudostratified epithelium. Similar epithelial types were observed in the *corpus*, while the *cauda* displayed predominantly pseudostratified epithelium, except in 48-month-old cats, which also showed exclusively pseudostratified epithelium. Intraepithelial cysts were observed in the epithelial duct of 24- and 48-month-old cats in all duct segments, except the *cauda*. These cysts were generally solitary, although occasionally double cysts were found both in the caput and *corpus* of the epididymis.

3.2. Growth patterns and morphometric analysis

Analysis of Table 1 illustrates a progressive increase in corpus weight and the volume of reproductive organs from 6 to 48 months of age. Corpus weight started at 3.0 kg ± 0,2 at six months and gradually ascended to 5.8 kg ± 0.7 at 48 months, highlighting statistically significant increments between evaluated growth stages. Testicular volume increased from 0.71 ml ± 0.33 to 2.15 ml ± 0.63 over the same period, with significant differences noted from 48 months compared to all previous age groups. Fig. 3 depicts the growth trajectory of corpus weight and organ volume in normal domestic cats over a 48-month period, showing a sustained and significant increase in corpus weight ($p < 0.0001$) and a significant increase in testicular volume ($p < 0.0025$). In contrast, while the volume of the epididymis also increased with age, its growth was less pronounced compared to corpus weight and testicular volume, though still statistically significant ($p < 0.0001$). These results indicate a positive and significant correlation between age

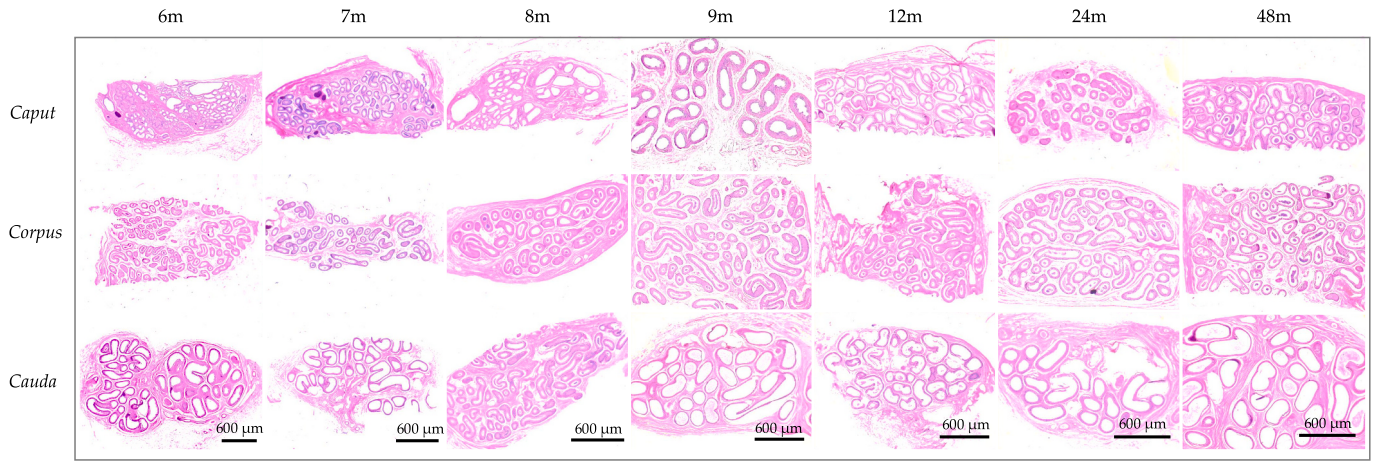

Fig. 2. Temporal sequence of histology in the *caput, corpus*, and cauda sections of the epididymis in domestic cats (*Felis silvestris catus*) at 6, 7, 8, 9, 12, 24, and 48 months of age. Bar: 600 µm.

Table 1
Body weight and organ volume by age (months). $n = 6$/age.

	6	7	8	9	12	24	48
Body weight (kg)	3.0 ± 0,2^{a,b,c,d}	3,9 ± 0.4^{e,f,g}	4,7 ± 0,4^{h,i,j}	5.2 ± 0,6^{a}	5,2 ± 0.5^{b,e,h}	5.8 ± 0.5^{c,f,i}	5.8 ± 0.7^{d,g,j}
Testis (ml)	0.71 ± 0.33^{a}	0.98 ± 0.36^{b}	1.01 ± 0.50^{c}	1.06 ± 0.46^{d}	1.18 ± 0.59^{e}	1.42 ± 0.53	2.15 ± 0.63^{a,b,c,d,e}
Epididymis (ml)	0.18 ± 0,074^{a}	0.19 ± 0.06^{b}	0.21 ± 0.10^{c}	0.29 ± 0.11^{d}	0.26 ± 0.10^{e}	0.31 ± 0.10	0.38 ± 0.15^{a,b,c,d,e}

Similar letters indicate statistical differences; $p < 0.05$. Statistical analyses were performed using ANOVA with Tukey's posthoc to identify significant differences between groups.

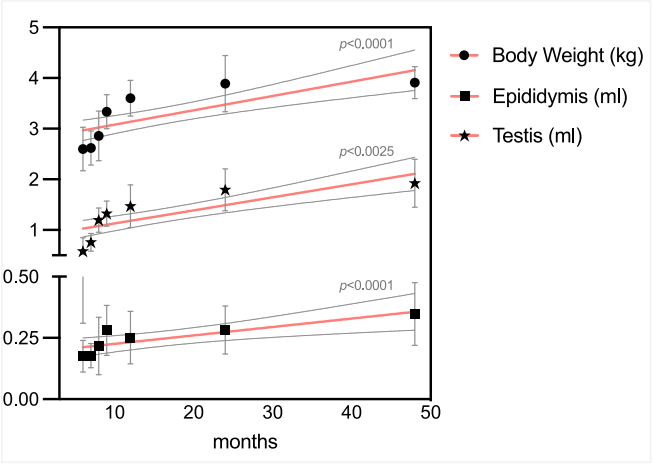

Fig. 3. Age-related progression of body weight, testicular volume, and epididymal volume in clinically normal domestic cats (*Felis silvestris catus*) between 6 and 48 months of age. Each graph presents mean values ± standard deviation per age group, with red lines indicating the simple linear regression and shaded areas representing the 95 % confidence intervals. Significant age-related increases were observed for body weight and testicular volume ($p < 0.0001$), and for epididymal volume ($p < 0.0025$), reflecting coordinated somatic and reproductive organ development during postnatal maturation. (For interpretation of the references to colour in this figure legend, the reader is referred to the web version of this article.)

and increases in both corpus weight and the volume of reproductive organs, with the changes being more notable in weight and testicular volume. The normality test confirmed that the data was normally distributed, allowing for the use of a parametric test for statistical analysis. Table 2 decaudas the evolution of linear morphometric variables in the *caput, corpus*, and *cauda* at each age. A general widening of the luminal diameter of the epididymal duct was observed across all age groups analyzed in this study. Values ranged from 30.84 ± 9.1 µm in the *caput* at six months to 252.4 ± 27.4 µm in the *cauda* at 48 months, reflecting a broad range of luminal expansion associated with developmental changes over time. Similarly, the height of the ductal epithelium demonstrated progressive and significant increases in the *caput, corpus,* and *cauda*, with growth noted from 25.88 ± 4.5 µm in the *caput* at six months to 39.64 ± 4.0 µm in the caput at 48 months. The height of the stereocilia also changed over time, though the increase was less pronounced compared to the other two variables, suggesting a continuous, statistically significant ($p < 0.05$), and distinct pattern of development in the epididymal structure.

3.3. Stereological variability and morphological changes

Variability was noted in the volume density of the ductal lumen (%$V_{V\ [DL]}$) across different sections and ages, with changes not following a uniform direction. For example, in the *caput*, the volume density (%) decreased from 29.2 ± 2.0 at six months to 18.5 ± 2.5 at 48 months. Conversely, in the *caput* and *cauda,* an increase was observed at 12 months, followed by a decrease at 48 months. The volume density of the ductal epithelium (%$V_{V[DE]}$) in the *caput* significantly increased from 31.1 ± 3.0 at six months to 39.6 ± 2.3 at 48 months, indicating a steady increase with age. The volume density of blood vessels (%$VV_{[BV]}$) exhibited slight incremental increases across all three sections analyzed, with the caput showing an increase from 1.4 ± 0.3 to 2.2 ± 0.8. The volume density of smooth muscle (%$V_{V\ [SM]}$) in the *caput* displayed minor variations with age, beginning at 15.7 ± 1.5 % at six months and slightly decreasing to 10.8 ± 2.1 % at 48 months. In the *caput*, the volume density started at 17.1 ± 1.4 % and decreased to 15.4 ± 4.2 % at 48 months. However, in the *cauda*, a more variable pattern emerged, starting from 30.5 ± 4.7 % at six months and decreasing to 21.8 ± 5.4 % at 48 months (Table 3).

3.4. Cellular composition and correlations

The relative proportion of principal cells (PCs), basal cells (BCs), and apical cells (ACs) in the *caput, caput*, and *cauda* across various ages (6, 7, 8, 9, 12, 24, and 48 months) are decaudaed in Table 4. PCs constituted

Table 2
Linear morphometric variables assessed in the different sections of the epididymal duct (caput, corpus, cauda) at the ages of 6, 7, 8, 9, 12, 24, and 48 months (n = 6/age). Measurements include luminal diameter (LD), height of the ductal epithelium (DEH), and height of the stereocilia (SCH), all expressed in micrometers (μm).

		6	7	8	9	12	24	48
LD [μm]	*Caput*	30.84 ± 9.1 ^{a,b,c,d,e,f}	55.99 ± 9.6^{a,g,h,i}	63.22 ± 30.6^{b}	69.24 ± 32.1^{c}	76.31 ± 14.2^{d,g}	79.9 ± 20.5^{e,h}	113.5 ± 20.9^{f,i}
	Corpus	65.28 ± 16.1^{a,b,c,d,e}	71.35 ± 18.7^{f,g,h}	86.01 ± 22.5^{a,i}	82.29 ± 17.4^{b}	88.33 ± 20.0^{c,f}	91.55 ± 26.4^{d,g}	103.4 ± 20.8^{e,h,i}
	Cauda	144.9 ± 47.4 ^{a,b,c,d,e,f}	194 ± 55.2^{a,f,g}	300.4 ± 93.2^{b,f,h,i}	220 ± 60.5^{c}	147.8 ± 29.2^{g,h}	175.6 ± 23.0^{d,i}	252.4 ± 27.4^{e}
DEH [μm]	*Caput*	25.88 ± 4.5^{a}	27.98 ± 3.9^{b}	30.89 ± 5.9	33.30 ± 7.8	31.71 ± 8.2	33.63 ± 12.3	35.75 ± 5.7^{a,b}
	Corpus	23.98 ± 6.5^{a,b,c,d,e}	28.49 ± 5.4^{f}	31.53 ± 5.8^{a,g}	33.49 ± 9.7^{b,f}	32.23 ± 5.7^{c}	34.32 ± 4.8^{d}	39.64 ± 4.0^{e,g}
	Cauda	29.22 ± 3.0	26.54 ± 4.2	24.96 ± 5.6	26.22 ± 4.0	26.96 ± 4.5	21.39 ± 2.7	14.91 ± 3.1
SCH [μm]	*Caput*	10.5 ± 2.64	7.4 ± 1.48	10.2 ± 3.13	12.9 ± 2.1	9.3 ± 1.86	9.5 1 ± 0.76	10.7 ± 2.73
	Corpus	4.8 ± 1.0	6.1 ± 1.7	7.8 ± 3.0	6.16 ± 1.2	7.2 ± 1.7	6.7 ± 1.6	5.7 ± 1.7
	Cauda	4.4 ± 1.6	5.0 ± 1.2	3.9 ± 1.7	5.7 ± 1.7	4.8 ± 1.5	3.0 ± 0.9	6.2 ± 1.3

Similar letters indicate statistical differences; $p < 0.05$. Statistical analyses were performed using ANOVA with Tukey's posthoc to identify significant differences between groups.

Table 3
Volume density of ductal lumen (DL), smooth muscle (SM), connective tissue (CT), ductal epithelium (DE), and blood vessels (BV) in caput, corpus and cauda of the epididymis at the ages of 6, 7, 8, 9, 12, 24, and 48 months (n = 6/age). Values are expressed as percentage of volume density (%Vv).

		6	7	8	9	12	24	48
$\%V_V$ [DL]	*Caput*	29.2 ± 2.0	23 ± 1.1^{a,b}	18.6 ± 3.1	18.2 ± 2.4	16.9 ± 1.4^{a}	16.3 ± 2.1^{b}	18.5 ± 2.5
	Corpus	17.2 ± 3.0^{a,b,c,d,e}	28.1 ± 2.8	31.5 ± 3.4^{a}	28.9 ± 3.7^{b}	30.6 ± 3.3^{c}	24.2 ± 2.0^{d}	22.9 ± 3.6^{e}
	Cauda	22.8 ± 4.1	27.1 ± 4.3	29.1 ± 2.8	26.6 ± 2.8	30.5 ± 2.2	32.4 ± 7.4	39.8 ± 7.7
$\%V_V$ [SM]	*Caput*	15.7 ± 1.5^{a,b}	19.8 ± 2.2	22.6 ± 2.2	25.5 ± 2.4^{a}	31.4 ± 1.9 ^{a}	15 ± 2.4	10.8 ± 2.1
	Corpus	17.1 ± 1.4	16.4 ± 2.7	15.7 ± 2.8	19.7 ± 2.7	23.2 ± 2.0	20.3 ± 3.8	21.8 ± 5.4
	Cauda	30.5 ± 4.7	23.6 ± 4.8	21.6 ± 5.2	24.2 ± 5.0	18.2 ± 3.7	23.4 ± 2.3	23.6 ± 2.3
$\%V_V$ [CT]	*Caput*	20.3 ± 1.8	23.1 ± 2.0	19.9 ± 3.2	25.5 ± 2.3	20.4 ± 3.0	22.2 ± 1.4	22.4 ± 2.1
	Corpus	25.8 ± 3.0	21.4 ± 2.7	18.3 ± 1.7	12.3 ± 2.5	12.6 ± 1.4	13.9 ± 3.2	15.4 ± 4.2
	Cauda	23.8 ± 1.7	22.2 ± 2.9	17.9 ± 4.7	16 ± 3.1	17.4 ± 1.9	19.2 ± 2.6	17.7 ± 1.9
$\%V_V$ [DE]	*Caput*	31.1 ± 3.0	33.3 ± 1.8^{a}	35.7 ± 2.7^{b}	37.5 ± 2.8	37.2 ± 1.9	38.2 ± 3.5	39.6 ± 2.3^{a,b}
	Corpus	25.6 ± 1.8^{a}	29.4 ± 2.6^{b}	24.9 ± 3.3	35.3 ± 2.5	36.9 ± 4.2	41.1 ± 2.b	43.6 ± 2.1^{a,b}
	Cauda	29.9 ± 9.2	29.3 ± 5.3	28.3 ± 1.5^{a}	26.4 ± 2.0^{b}	25.7 ± 1.6	25.8 ± 5.3	31.4 ± 2.0^{a,b}
$\%V_V$ [BV]	*Caput*	1.4 ± 0.3	2.3 ± 0.9	2.3 ± 0.7	2.0 ± 1.0	2 ± 1.2	2.2 ± 0.6	2.2 ± 0.8
	Corpus	1.7 ± 0.6	1.4 ± 0.5	1.9 ± 1.0	1.7 ± 0.7	1.6 ± 0.7	1.5 ± 0.8	1.8 ± 0.7
	Cauda	2.4 ± 1.2	2.0 ± 1.1	1.6 ± 0.6	1.4 ± 0.7	1.4 ± 0.7	2.1 ± 1.1	2.6 ± 0.9

Similar letters indicate statistical differences; $p < 0.05$. Statistical analyses were performed using ANOVA with Tukey's posthoc to identify significant differences between groups.

Table 4
Relative proportion of principal cells (PC), basal cells (BC), and apical cells (AC) in the various sections of the epididymal duct (caput, corpus and cauda) at the ages of 6, 7, 8, 9, 12, 24, and 48 months (n = 6/age).

		6	7	8	9	12	24	48
PC [%]	*Caput*	91.2 ± 2.2^{a}	85.6 ± 0.9	89.4 ± 2.3	89.2 ± 2.6^{a}	90.4 ± 2.2	88.2 ± 2.6	89 ± 2.0
	Corpus	87.8 ± 2.2	84.2 ± 4.9	85.4 ± 1.1	84.6 ± 3.6	85.8 ± 2.4	87.4 ± 2.1	85.4 ± 1.8
	Cauda	87.6 ± 1.5	85.2 ± 3.3^{a,b}	87.6 ± 1.7	89.6 ± 3.4^{a}	89.4 ± 3.4^{b}	85.6 ± 1.5	86.4 ± 1.5
AC [%]	*Caput*	5.2 ± 1.5	4.8 ± 1.3	4.0 ± 1.0	4.2 ± 1.3	3.0 ± 1.6	3.2 ± 1.6	3.6 ± 0.9
	Corpus	4.8 ± 1.6	3.4 ± 2.6	2.6 ± 1.3	5.2 ± 1.5	3.0 ± 1.2	5.4 ± 1.9	3.8 ± 1.3
	Cauda	2.2 ± 0.8	5.5 ± 3.0	3.8 ± 1.3	2.8 ± 0.5	2.3 ± 1.2	4.8 ± 1.5	3.6 ± 1.1
BC [%]	*Caput*	3.6 ± 1.0^{a,b}	9.6 ± 0.9	6.6 ± 1.5^{a}	6.6 ± 1.7^{b}	6.6 ± 1.1	8.6 ± 4.0	7.4 ± 2.7
	Corpus	7.4 ± 1.1^{a,b}	12.4 ± 3.6^{a}	12 ± 1.4^{b}	10.2 ± 2.3	11.2 ± 1.8	7.2 ± 2.4	10.8 ± 2.3
	Cauda	10.2 ± 1.3	10.4 ± 1.1	8. 6 ± 1.5	8.2 ± 2.8	9.2 ± 2.8	9.6 ± 1.1	10 ± 1.9

Similar letters indicate statistical differences; $p < 0.05$. Statistical analyses were performed using ANOVA with Tukey's posthoc to identify significant differences between groups.

most of the cell population at all ages and sections, with a slight decrease from 91.2 ± 2.2 % in the *caput* at six months to 89 ± 2.0 % at 48 months. Basal cells (BCs) displayed a variable pattern, with a marked increase in the *caput* and *cauda*, rising from 7.4 ± 1.1 % and 10.2 ± 1.3 %, respectively, at six months, to 10.8 ± 2.3 % and 10 ± 1.9 % at 48 months. ACs remained in low proportions compared to other cell types, changing slightly with age. These patterns indicate a relative stability in the proportion of PCs with a potential increase in BCs as age advances, which may reflect changes in cellular dynamics and epididymal function during maturation. Statistically significant differences ($p < 0.05$) between ages and sections highlight the complexity of cell composition and its evolution over time. Additionally, the r-Pearson correlation between age and morphological variables measured in the epididymis is described in Table 5. A positive and highly significant correlation ($r = 0.9324$, $p < 0.01$) was observed between age and the $\%V_{V\ [DL]}$ in the *cauda*, indicating an increase in luminal space with age in this region. In contrast, the $\%V_{V\ [SM]}$ in the *caput* showed a significant negative correlation ($r = -0.6167$, $p < 0.05$), suggesting a decrease in smooth muscle proportion with age in this section. Interestingly, the luminal diameter (LD) exhibited a strong positive correlation with age in the *caput* ($r = 0.8501$, $p < 0.05$), while no significant correlations were found for the height of the ductal epithelium (DEH) and the height of the stereocilia (SCH) in any region (*caput, corpus, cauda)*. These findings indicate specific early age-related changes in the structure of the epididymis that may correlate with functional changes in this organ throughout the development of domestic cats.

Table 5
r-Pearson correlation between age and morphological variables measured in epididymis (caput, corpus and cauda) of domestic cats. DL: Ductal lumen; SM: Smooth muscle; CT: Connective tissue; DE: Ductal epithelium; BV: Blood vessels; LD: lumen diameter; DEH: ductal epithelium height; SCH: stereocilia height.

	Age vs. $\%V_V$[DA]	Age vs. $\%V_V$[SM]	Age vs. $\%V_V$[CT]	Age vs. $\%V_V$[DE]	Age vs. $\%V_V$[BV]	Age vs. LD	Age vs. DEH	Age vs. SCH
Caput	−0.3836	−0.6167	0.1048	0.7121*	0.2829	0.8501*	0.3827	0.7239
Corpus	−0.2711	0.5638	−0.3543	0.8013*	0.2779	0.8254*	−0.03915	−0.1582
Cauda	0.9324**	−0.1073	−0.3114	−0.9531***	0.5837	0.3448	−0.139	0.4815

p-values ≤0.05 (*), ≤ 0.01(**), < 0.001(***).

4. Discussion

Reproductive biology in the Felidae family, especially concerning early-life changes, remains underexplored. This study, focusing on the domestic cat, pioneers a comprehensive stereological approach to the epididymis, providing novel quantitative data on morphological changes during the first 48 months of life. The life stages of the cat have been categorized into kitten (0–6 months), junior (7 months–2 years), adult (3–6 years), mature (7–10 years), senior (11–14 years) and geriatric (15+ years) (Hoyumpa Vogt et al., 2010). Our work focused on the kitten and junior life stages, investigating key developmental changes that occur during these critical early periods. By examining these stages in decauda, our findings provide a deeper understanding of the transitions into early adulthood in Felidae, offering valuable insights into their reproductive biology. Furthermore, this research aligns with the growing emphasis on multidisciplinary approaches, such as assisted reproductive technologies (ARTs), for the conservation of wild felines (Kochan et al., 2019; Thongphakdee et al., 2020), positioning the domestic cat as a model for endangered species conservation efforts.

The application of advanced stereological techniques to quantify epididymal changes represents a novel methodological contribution. Techniques such as minimizing tissue shrinkage artifacts (Dorph-Petersen et al., 2001), calibrating microtome block advance, and measuring section thickness at multiple points with a micrometer ensured precise volumetric data. Samples were processed in batches of no more than five, adhering to consistent intervals for collection, fixation, and processing. Verification steps and uniform random sampling-maintained accuracy, keeping the coefficient of error (CE) below 5 % (West, 2013), resulting in reliable and unbiased estimates.

To contextualize the morphometric and stereological findings within a functional framework, it is important to consider their biological implications. The observed increase in ductal epithelial height, particularly in the *caput epididymidis*, aligns with its established role in the active maturation and modification of spermatozoa during transit. This epithelial hypertrophy likely reflects heightened secretory and absorptive activity essential for creating the luminal environment necessary for sperm functional competence. Concurrently, the progressive accumulation of spermatozoa across all regions—especially the *cauda*—indicates the establishment of effective sperm storage capacity, a hallmark of reproductive maturation. These structural transformations, therefore, not only represent morphological development but also highlight critical adaptations of the epididymis that support its roles in sperm maturation, transport, and storage during the transition from puberty to reproductive maturity. Our findings on spermatozoa distribution across epididymal regions at different ages align with previous reports describing early accumulation in the *cauda* epididymidis, followed by a more homogeneous distribution throughout the epididymis by 48 months, coinciding with the onset of consistent testicular sperm production (Tsutsui et al., 2004). This pattern paralleled morphometric changes, including a progressive increase in ductal area and epithelial volume, particularly in the *caput*, which is histologically consistent with its role in sperm maturation. Conversely, the *cauda* displayed greater epithelial variability and relative volumetric reduction, which may reflect its capacity to modulate sperm storage in response to reproductive activity (Axnér, 2006). These observations reinforce the functional compartmentalization of the epididymis in the domestic cat, wherein the *caput* is specialized for sperm maturation and the *cauda* for storage and highlight how regional morphological adaptations support these physiological processes (Tsutsui et al., 2004; James et al., 2020a, b). These morphological changes are critical for maintaining reproductive health. The observed transformations in the duct of the epididymis are indicative of their essential function in spermatozoa maturation and storage, driven by age-related physiological and hormonal shifts.

Our stereological analysis revealed region-specific variations in the ductal epithelium, which comprised at least 30 % of the epididymal parenchyma across all age groups, increasing to 40 % and 50 % in the *caput* at 24 and 48 months, respectively. In contrast, the *cauda* showed a reduction to approximately 10 % of the parenchyma by 48 months. The increased epithelial volume in the *caput* suggests enhanced cellular proliferation to support sperm maturation and transport, consistent with its role in early sperm processing. While hormonal influences, cellular renewal, or reproductive activity could contribute to these changes, as noted in prior studies (Axnér, 2006), our study focused on morphological and stereological outcomes without hormonal data. Thus, we interpret these variations as evidence of region-specific remodeling in the feline epididymis, with the observed epithelial proportions highlighting developmental adaptations. Future research integrating hormonal and functional analyses could further clarify the drivers of these morphological differences. On the other hand, the reduction in epithelial proportion in the *cauda* suggests a predominant focus on sperm storage as they mature and are prepared for ejaculation.

Intraepithelial cysts identified in the *caput* and *corpus epididymidis* of cats aged 24 to 48 months were incidental histological findings in clinically healthy individuals, representing age-related morphological variations not previously described in this species with such regional detail. While epididymal cysts have been rarely reported in felines—such as the isolated case described by Hill et al. (2024) in the *caput* of an 8-month-old cat—our observations suggest that these lesions may have broader spatial distribution and could reflect a wider spectrum of developmental anomalies, potentially linked to alterations in the *rete testis*. Comparable structures have been described in rams and humans (Costa et al., 2007; Nistal et al., 1990), and in human infants, their presence has been associated with interstitial endocrine cell tumors, implicating possible hormonal influences (James et al., 2020a, b; Asensio Lahoz and Martínez Bretones, 1997). Although hormonal profiles were not assessed in the present study, the consistent appearance of these cysts in older individuals supports the notion that they may result from cumulative structural adaptations or dysgenetic changes associated with aging. Further studies incorporating hormonal analyses would be valuable to explore the underlying mechanisms of cyst formation in feline epididymal tissue. Additionally, the occurrence of these cysts in multiple regions underscores the need for further research to elucidate their etiology, whether developmental or trauma-related, and their potential implications for reproductive health in felids.

Our study revealed significant age-related and regional variations in ductal epithelial height across epididymal regions. While the *caput* nearly doubled in height by 48 months compared to 6 months, the *cauda* exhibited a continuous reduction, reaching half its initial height by 48 months. Supported. These regional differences are consistent with rodent models, where testosterone, cytokines, and growth factors such as EGF and bFGF regulate epithelial proliferation and differentiation (Hamzeh and Robaire, 2009). The increased height in the *caput* suggests

greater functional demands for sperm maturation and transport, driven by elevated testosterone and growth factors. In contrast, the cauda's reduced epithelial height reflects a shift toward storage-focused functionality. Differences in aquaporin activity and cellular metabolism may explain the variations in stereocilia length in feline epididymis (Schön et al., 2009; Oliveira et al., 2005). Similar patterns in canines highlight androgen-regulated aquaporins, as shown in nandrolone decanoate-treated rats (Squillacioti et al., 2021). In humans and felines, testosterone and growth factors like EGF and bFGF play crucial roles in epididymal differentiation (Tsutsui et al., 2004; Cornwall, 2009; Fujihara et al., 2014). EGF enhances spermatogenesis and follicular viability in felines, while bFGF and TGF-beta contribute to tissue development and regional morphometric changes (Cross and Dexter, 1991; Breton et al., 2019a, b). These findings underscore the significance of these factors in epididymal development, though further research is needed for domestic cats.

Principal cells were predominant across all epididymal regions, outnumbering basal and apical cells, consistent with their essential role in regulating the luminal microenvironment via paracrine signaling (Axnér et al., 1999; Sánchez et al., 1998). The stability in principal cell numbers from 6 to 48 months suggests early sexual maturity in domestic cats, aligning with their role in secreting substances critical for sperm maturation (Gutiérrez-Reinoso and García-Herreros, 2016). Basal cells, though less numerous, play a key role in sensing luminal changes through axiopodia, modulating adjacent cells' activity—a function observed in viscacha and humans (Cruceño et al., 2017; Breton et al., 2019a, b). Apical cells contribute to luminal pH regulation via proton secretion (Park et al., 2017). While pH levels were not measured here, these cells are crucial for creating optimal conditions for sperm maturation and storage. The sustained population and activity of principal cells suggest hormonal regulation, as seen in species like the Egyptian dromedary (Ibrahim and Abdel-Maksoud, 2019). Regional specialization and cellular functions in the human proximal epididymis also highlight the roles of principal, basal, and apical cells (Leir et al., 2020). Additionally, androgen and estrogen receptor immunolocalization in rats supports hormonal regulation of these cells' distribution and function (Menad et al., 2021). Insights gained from other species provide valuable information on the need to understand the early dynamics and functions of the various cell types within the epididymis of domestic cats. This highlights the complexity of this organ in its critical role in sperm maturation and the regulation of the luminal microenvironment.

The stereological study revealed significant tissue ratio changes in the epididymis over 48 months, particularly in the corporal region, highlighting the combined effects of aging and hormonal factors on epididymal morphology. The increase in volumetric density of the ductal epithelium with age suggests an adaptive response to greater functional demands, likely regulated by hormones. A consistent pattern in the volumetric density of the ductal lumen across *caput* regions, and its initial increase followed by stabilization in the corporal region, corresponds to the onset of sexual activity and efficient sperm maturation by 12 months. The stabilization at 24 and 48 months indicates a steady state of epididymal function. The increase in ductal epithelium height and cilia reflects the ducts' readiness for secretory and absorptive functions, important for maintaining the environment needed for sperm maturation. Additionally, the absence of significant changes in smooth muscle and blood vessels in the *caput*, along with the reduced connective tissue area in the corporal and caudal regions, highlights the region-specific remodeling driven by androgens. This is supported by studies demonstrating that epididymal development and ductal function are androgen-dependent, initiated by the testosterone peak in humans (Axnér, 2006). The interplay between structural maturation and hormonal regulation is evident in the increased density of the ductal epithelium and changes in connective tissue. Androgens play a pivotal role, as demonstrated by the significance of androgen and vitamin D receptors in the epididymis (Wang et al., 2021). The predominant localization of androgen receptors in principal cells, particularly in the *corpus* and *cauda*, highlights their influence on epididymal morphology and function. Testosterone's role in synthesizing epididymal proteins further underscores the importance of androgens in maintaining structural integrity and functional capacity (Sullivan and Mieusset, 2016). Aging introduces histological changes and reduced protein synthesis, potentially impacting sperm maturation and epididymal structure (López-Trinidad et al., 2021). Given the limited data on domestic cats, insights from human studies provide valuable context, elucidating androgen-mediated mechanisms, ductal epithelial regulation, and age-related adaptations (Wang et al., 2021; Nicander and Plöen, 1979). The proposed role of androgens in epididymal maturation is supported by our stereological findings, which revealed a marked increase in the volumetric density of the ductal epithelium in the *caput* between 6 and 12 months of age, coinciding with the post-pubertal rise in testicular androgen production. In contrast, a relative increase in luminal volume observed in older individuals may reflect enhanced sperm storage capacity in the *cauda*. These region-specific changes reinforce the interpretation that androgenic signaling contributes to differential structural remodeling of the epididymis, facilitating its functional specialization during sexual maturation. These findings inform hypotheses and guide future research on the unique features of the cat's epididymis.

4.1. Limitations and future directions

While this study provides valuable morphometric and morphological data on the epididymis of domestic cats, certain methodological limitations should be considered. The cross-sectional design, though informative, restricts the ability to track individual developmental trajectories or establish causal relationships between age and histological changes. Additionally, potential variability in tissue processing—despite the use of automated histological protocols—may have introduced minor inconsistencies due to handling or batch effects. Although androgenic influence is suggested, the absence of molecular analyses limits the interpretation of hormonal regulation. Future studies should include longitudinal designs to better capture individual variation over time and incorporate molecular approaches to assess the expression of hormonal receptors and functional proteins, such as aquaporins, which are critical for epididymal function. These strategies will enhance understanding of the mechanisms underlying structural maturation and their implications for reproductive health and assisted reproduction in felids.

Finally, this study, through the application of stereological and morphometric techniques, provides detailed insights into age-related epididymal changes in domestic cats, supporting their use as a translational model for wild felids in the context of assisted reproductive technologies (ART) (Thongphakdee et al., 2020). The observed regional variations in epithelial height—particularly the increase in the *caput* and reduction in the *cauda*—as well as the identification of intraepithelial cysts in older individuals, offer valuable structural parameters for optimizing epididymal sperm extraction and cryopreservation protocols. These morphological markers inform critical decisions regarding the timing and anatomical targeting of sperm retrieval in both domestic and wild felids, particularly in postmortem or time-sensitive conservation scenarios. Thus, our findings contribute essential anatomical knowledge to enhance the precision and success of ART strategies aimed at preserving endangered feline species.

5. Conclusion

This study demonstrates marked age-related morphological changes in the epididymis of the domestic cat (*Felis silvestris catus*) during the first 48 months of life, particularly an increase in epithelial volume density in the *caput* region. These findings suggest a progressive structural maturation associated with sexual development and potentially modulated by androgenic influence. The predominance of principal cells across regions reinforces their functional significance in luminal regulation and

sperm maturation. While stereological and microscopy techniques proved effective, the study acknowledges methodological limitations inherent to cross-sectional designs. Overall, this work contributes foundational quantitative data on feline epididymal development and underscores the relevance of hormonal and cellular dynamics in reproductive tract maturation.

Data sharing

The data that support the findings of this study are available from the corresponding author upon reasonable request.

CRediT authorship contribution statement

P. Salinas: Writing – review & editing, Writing – original draft, Visualization, Supervision, Resources, Methodology, Investigation, Formal analysis, Conceptualization. **D. Escobar:** Writing – review & editing, Writing – original draft, Visualization, Methodology, Investigation, Formal analysis, Conceptualization.

Declaration of generative AI and AI-assisted technologies in the writing process

Generative AI and AI-assisted technologies should only be used in the writing process to improve the readability and language of the manuscript.

Declaration of competing interest

The authors declare that they have no known competing financial interests or personal relationships that could have appeared to influence the work reported in this paper.

References

Asensio Lahoz, L.A., Martínez Bretones, F., 1997. Tumor de células de Leydig asociado a quiste epididimario [Leydig cell tumor associated with epididymal cyst]. Actas Urol. Esp. 21 (5), 487–488.

Axnér, E., 2006. Sperm maturation in domestic cat. Theriogenology 66 (1), 14–24. https://doi.org/10.1016/j.theriogenology.2006.03.022.

Axnér, E., Malmqvist, M., Linde-Forsberg, C., Rodriguez-Martinez, H., 1999. Regional histology of ductus epididymidis in domestic cat. J. Reprod. Dev. 45 (2), 151–160. https://doi.org/10.1262/jrd.45.151.

Bellows, J., Center, S., Daristotle, L., Estrada, A.H., Flickinger, E.A., Horwitz, D.F., Lascelles, B.D., Lepine, A., Perea, S., Scherk, M., Shoveller, A.K., 2016. Evaluating aging in cats: how to determine what is healthy and what is disease. J. Feline Med. Surg. 18 (7), 551–570. https://doi.org/10.1177/1098612X16649525.

Breton, S., Nair, A.V., Battistone, M.A., 2019. Epithelial dynamics in epididymis: role in sperm maturation, protection, and storage. Andrology 7 (5), 631–643. https://doi.org/10.1111/andr.12632.

Cornwall, G.A., 2009. New insights into Epididymal biology and function. Hum. Reprod. Update 15 (2), 213–227. https://doi.org/10.1093/humupd/dmn055.

Costa, F.L.A., Silva, S.M.M.S., Nascimento, E.F., 2007. Pathologic evaluation of testis and epididymis of hairy rams in the semi-arid region of Piaui state. Arq. Brasil. Med. Vet. Zoot. 59 (5), 1110–1116. https://doi.org/10.1590/S0102-09352007000500004.

Cross, M., Dexter, T., 1991. Growth factors in development, transformation, and tumorigenesis. Cell 64, 271–280. https://doi.org/10.1016/0092-8674(91)90638-F.

Cruceño, A.A., Aguilera-Merlo, C.I., Chaves, E.M., Mohamed, F.H., 2017. Epididymis of Viscacha (*Lagostomus maximus maximus*): a morphological comparative study in relation to sexual maturity. Anat. Histol. Embryol. 46 (1), 73–84. https://doi.org/10.1111/ahe.12240.

Dorph-Petersen, K.A., Nyengaard, J.R., Gundersen, H.J., 2001. Tissue shrinkage estimation in stereology. J. Microsc. 204, 232–246.

Fleming, P., Crawford, H., Auckland, C., Calver, M., 2021. Nine ways to score nine lives – identifying appropriate methods to age domestic cats (*Felis catus*). J. Zool. 314, 211–226. https://doi.org/10.1111/jzo.12869.

Fujihara, M., Comizzoli, P., Keefer, C.L., Wildt, D.E., Songsasen, N., 2014. Epidermal growth factor (EGF) sustains in vitro primordial follicle viability by enhancing stromal cell proliferation via MAPK and PI3K pathways in the prepubertal, but not adult, cat ovary. Biol. Reprod. 90 (4), 86. https://doi.org/10.1095/biolreprod.113.115089.

Geuna, S., Herrera-Rincon, C., 2015. Update on stereology for light microscopy. Cell Tissue Res. 360 (1), 5–12.

Gundersen, H.J., Bendtsen, T.F., Korbo, L., Marcussen, N., Møller, A., Nielsen, K., Nyengaard, J.R., Pakkenberg, B., Sørensen, F.B., Vesterby, A., 1988. Some new, simple and efficient stereological methods and their use in pathological research and diagnosis. Acta Pathol. Microbiol. Immunol. Scand. 96 (5), 379–394. https://doi.org/10.1111/j.1699-0463.1988.tb05320.x.

Gutiérrez-Reinoso, M.A., García-Herreros, M., 2016. Normozoospermic versus teratozoospermic domestic cats: differential testicular volume, sperm morphometry, and subpopulation structure during epididymal maturation. Asian J. Androl. 18 (6), 871–878. https://doi.org/10.4103/1008-682X.187583.

Hamzeh, M., Robaire, B., 2009. Testosterone effect on rat Epididymal epithelium. J. Androl. 30, 200–212. https://doi.org/10.2164/jandrol.108.006171.

Hill, F.I., Tse, M.P., Mills, S.W., Sandy, J.R., Elsohaby, I., Barrs, V.R., 2024. Histopathological changes in testicular lesions in cats. J. Feline Med. Surg. 26 (9), 1098612X241264124. https://doi.org/10.1177/1098612X241264124.

Hoyumpa Vogt, A., Rodan, I., Brown, M., Brown, S., Buffington, C.A., Larue Forman, Neilson, J., Sparkes, A., 2010. AAFP-AAHA: feline life stage guidelines. J. Feline Med. Surg. 12 (1), 43–54. https://doi.org/10.1016/j.jfms.2009.12.006.

Ibrahim, D., Abdel-Maksoud, F.M., 2019. Immunohistochemical and ultrastructural features of the seasonal changes in the Epididymal epithelium of camel (*Camelus dromedarius*). Microsc. Microanal. 25 (5), 1273–1282. https://doi.org/10.1017/S1431927619014843.

International Committee on Veterinary Gross Anatomical Nomenclature (ICVGAN), 2017. Nomina Anatomica Veterinaria, 6th ed. Editorial Committee Hanover, World Association of Veterinary Anatomists, Germany. Available from: https://www.wava-amav.org/downloads/nav_6_2017.zip.

International Committee on Veterinary Histological Nomenclature (ICVHN), 2017. Nomina Histologica Veterinaria. World Association of Veterinary Anatomists. Available from: https://www.wava-amav.org/downloads/NHV_2017.pdf.

James, E.R., Carrell, D.T., Aston, K.I., Jenkins, T.G., Yeste, M., Salas-Huetos, A., 2020. The role of the epididymis and the contribution of Epididymosomes to mammalian reproduction. Int. J. Mol. Sci. 21 (15), 5377. https://doi.org/10.3390/ijms21155377.

Johnson, L., Neaves, W.B., 1981. Age changes in stallion testis. Biol. Reprod. 24, 703–712.

Kochan, J., Nižański, W., Moreira, N., Cubas, Z.S., Nowak, A., Prochowska, S., Partyka, A., Młodawska, W., Skotnicki, J., 2019. ARTs in wild felid conservation programmes in Poland and in the world. J. Vet. Res. 63 (3), 457–464. https://doi.org/10.2478/jvetres-2019-0043.

Leir, S.H., Yin, S., Kerschner, J.L., Cosme, W., Harris, A., 2020. An atlas of human proximal epididymis reveals cell-specific functions and distinct roles for CFTR. Life Sci. Alliance 3 (11), e202000744. https://doi.org/10.26508/lsa.202000744.

López-Trinidad, B.P., Vigueras-Villaseñor, R.M., Konigsberg, M., Ávalos-Rodríguez, A., Rodríguez-Tobón, A., Cortés-Barberena, E., Arteaga-Silva, M., Arenas-Ríos, E., 2021. Alterations in epididymal sperm maturation caused by ageing. Reprod. Fertil. Dev. 33 (18), 855–864. https://doi.org/10.1071/RD21081.

Malmqvist, M., 1978. Regional cytology of cat Epididymal duct. J. Ultrastruct. Res. 63 (abstract 96).

Menad, R., Fernini, M., Lakabi, L., Smaï, S., Gernigon-Spychalowicz, T., Farida, K., Bonnet, X., Moudilou, E., Exbrayat, J.M., 2021. Androgen and estrogen receptors immunolocalization in the sand rat (*Psammomys Obesus*) cauda epididymis. Acta Histochem. 123 (2), 151683. https://doi.org/10.1016/j.acthis.2021.151683.

National Research Council (US) Committee, 2011. Guide for Care and Use of Laboratory Animals, 8th ed. National Academies Press (US), Washington (DC). Available from: https://www.ncbi.nlm.nih.gov/books/NBK54050.

Nicander, L., Plöen, L., 1979. Studies on regional fine structure and function in rabbit epididymis. Int. J. Androl. 2, 463–481. https://doi.org/10.1111/j.1365-2605.1979.tb00078.x.

Nistal, M., Iñiguez, L., Paniagua, R., 1990. Pitted pattern in the human epididymis. J. Reprod. Fertil. 89 (2), 655–661. https://doi.org/10.1530/jrf.0.0890655.

Oliveira, C.A., Carnes, K., França, L.R., Hermo, L., Hess, R.A., 2005. Aquaporin-1 and -9 differentially regulated by oestrogen in efferent ductule epithelium. Biol. Cell. 97, 385–395. https://doi.org/10.1042/BC20040078.

Park, Y.J., Battistone, M.A., Kim, B., Breton, S., 2017. Relative contribution of clear cells and principal cells to luminal pH in the mouse epididymis. Biol. Reprod. 96 (2), 366–375. https://doi.org/10.1095/biolreprod.116.144857.

Pintus, E., Kadlec, M., Karlasová, B., Popelka, M., Ros-Santaella, J.L., 2021. Spermatogenic activity and sperm traits in post-pubertal and adult tomcats (*Felis catus*): implication of intra-male variation in sperm size. Cells 10 (3), 624. https://doi.org/10.3390/cells10030624.

Sánchez, B., Flores, J.M., Pizarro, M., García, P., 1998. Histological and immunohistochemical study of the cat epididymis. Anat. Histol. Embryol. 27 (2), 135–140. https://doi.org/10.1111/j.1439-0264.1998.tb00169.x.

Schön, J., Neumann, S., Wildt, D.E., Pukazhenthi, B.S., Jewgenow, K., 2009. Localization of oestrogen receptors in the epididymis during sexual maturation of the domestic cat. Reprod. Domest. Anim. 44 Suppl 2, 294–301. https://doi.org/10.1111/j.1439-0531.2009.01391.x.

Smith, L.B., Walker, W.H., 2014. The regulation of spermatogenesis by androgens. Semin. Cell Dev. Biol. 30, 2–13. https://doi.org/10.1016/j.semcdb.2014.02.012.

Sowińska, N., 2021. Kot Domowy Jako model Badawczy w Procedurach Wspomaganego Rozrodu Dzikich Kotowatych [the domestic cat as a research model in the assisted reproduction procedures of wild felids]. Postepy Biochem. 67 (4), 362–369. https://doi.org/10.18388/pb.2021_416.

Squillacioti, C., Mirabella, N., Liguori, G., Germano, G., Pelagalli, A., 2021. Aquaporins differentially regulated in canine cryptorchid efferent ductules and epididymis. Animals 11. https://doi.org/10.3390/ani11061539.

Sullivan, R., Mieusset, R., 2016. The human epididymis: its function in sperm maturation. Hum. Reprod. Update 22, 574–587. https://doi.org/10.1093/humupd/dmw015.

Thongphakdee, A., Sukparangsi, W., Comizzoli, P., Chatdarong, K., 2020. Reproductive biology and biotechnologies in wild felids. Theriogenology 150, 360–373. https://doi.org/10.1016/j.theriogenology.2020.02.004.

Tschanz, S.A., Burri, P.H., Weibel, E.R., 2011. STEPanizer: tool for stereology of digital images. J. Microsc. 243, 47–59.

Tsutsui, T., Kuwabara, S., Kuwabara, K., Kugota, Y., Kinjo, T., Hori, T., 2004. Development of Spermatogenic function in the sex maturation process in male cats. J. Vet. Med. Sci. 66 (9), 1125–1127. https://doi.org/10.1292/jvms.66.1125.

Wang, T.E., Minabe, S., Matsuda, F., Li, S.H., Tsukamura, H., Maeda, K.I., Smith, L., O'Hara, L., Gadella, B.M., Tsai, P.S., 2021. Testosterone regulation on quiescin sulfhydryl oxidase 2 synthesis in the epididymis. Reproduction 161 (5), 593–602. https://doi.org/10.1530/REP-20-0629.

West, M.J., 2013. Tissue shrinkage and stereological studies. Cold Spring Harb Protoc 2013 (3), top071860. https://doi.org/10.1101/pdb.top071860.